

## Sub-L<sub>1</sub> Norm Regularized Inversion Deblending in Local 3D FK Domain for Ocean Bottom Node Data

*Jun Sun\*, Zhaojun Liu, Manhong Guo, Graeme Stock, Bin Wang (TGS)*

### Summary

Inversion deblending in a sparse transformed domain is an important approach to obtain high quality deblended data for simultaneous source acquisition. For ocean bottom node data, more than one vessel with multiple sources are used to reduce acquisition duration and increase shot density, but the increased blending fold tends to make the inversion solution unstable and less accurate. We present a new method and some tips to improve the stability and accuracy of inversion deblending for node data and demonstrate application on two different surveys.

This new method uses sub-L<sub>1</sub> norm for regularization in the objective function, the Iterative Shrinkage-Thresholding Algorithm (ISTA) to solve for the deblended model, and time-variant local 3D FK transform to promote sparsity. Some pointers for improving deblending performance on field data are provided as well.

### Introduction

Ocean bottom node (OBN) acquisition can provide long offset, wide azimuth and clean data at low frequencies, so it becomes more powerful for FWI and subsalt imaging. However, an OBN survey is more expensive compared with a streamer survey. The nodes sometimes need to be pulled out to recharge and redeploy if the acquisition period is too long, which makes the cost even higher.

Recently simultaneous sourcing is playing a key role in reducing survey duration as well as increasing the shot density (Beasley et al., 1998; Berkhouit, 2008; Abma and Foster, 2020). The delay times between the sources are dithered so that interference from other simultaneous sources appear as random noise in domains other than the shot domain. We utilize this fact to remove the blending noise and recover the deblended model.

There are two main categories of deblending methods for simultaneous source data. The first one is denoising by filtering out the incoherent signal from other sources as noise in a domain other than shot (Akerberg et al., 2008; Moore et al., 2008; Mahdad et al., 2011; Abma et al., 2012; Zhan et al., 2015; Xuan et al., 2020). This kind of method is fast and can achieve good quality on migration images. However, if investigated closely, damage to the primary energy and residual blending sources can be found in pre-stack gathers. Therefore, a second approach to deblending of sparse inversion (Abma and Yan, 2009; Abma et al., 2010; Chen et al., 2014; Kumar and Hampson, 2020; Liu et al.,

2014; Peng and Meng, 2016; Masoomzadeh et al., 2018; Qu et al., 2016) has been developed: calculate the desired deblended or unblended model by inverting the forward blending operator and applying it on the measured blended data. This is normally implemented by iteratively inverting the operator with an assumed sparsity constraint for regularization rather than direct inversion, due to computational complexity.

The inversion deblending method has its own drawbacks, however. It is much more time consuming than a denoising method. Additionally, if the blending fold is high, it tends to be unstable and less accurate (Abma et al., 2015). In general, the inversion deblending method is stable for marine data as blending fold is relatively low (<5). In OBN simultaneous sourcing surveys, however, to save cost the number of sources is increased up to 6 or even more (Ramirez et al., 2021). The resulting high blending fold presents challenges to our inversion method on convergence, recovering weak events in areas with strong blending noise, and high fidelity preservation on direct arrivals and diving waves. It demands an efficient, highly accurate and stable algorithm.

In this abstract, we will present our new inversion deblending methods (Sun et al., 2022) which improve the stability and accuracy of the deblending process over our previous FK domain approach (Masoomzadeh et al., 2019). We will show two field data examples that demonstrate the efficacy of these new ideas.

### Methods

A blended data of simultaneous sources can be represented using Berkhouit's (Berkhouit, 2008) formulation,

$$D = \Gamma m, \quad (1)$$

where  $\Gamma$  is the blending operator,  $D$  is the recorded data, and  $m$  is the desired deblended records. If we formulate the deblending problem just as a least square problem, then the system is underdetermined and has multiple solutions. To reach a unique solution, the constraint of sparsity in a transformed domain is added. The deblending problem is now formulated into minimizing an objective function with a least square term and a regularization term of L<sub>P</sub> (0 < P < 1) norm (Qu et al 2016) as

$$f(m) = \|D - \Gamma m\|_2 + \alpha \|S^{-1}m\|_P, \quad (2)$$

where  $f(m)$  is the objective function to minimize,  $\|\dots\|$  is the norm calculation,  $\alpha$  is a scalar weighting the regularization

## Sub-L<sub>1</sub> Norm Regularized Inversion Deblending in Local 3D FK Domain for OBN Data

term and  $S^{-1}$  is a sparsity-promoted transform. The regularization term forces the sparsest solution in the transformed domain in a sub-L<sub>1</sub> norm sense.

The well-known ISTA method is used to solve this regularized least square problem and in deblending it can be written as

$$\mathbf{m}_{k+1} = S T_{\tau,P} S^{-1} [\mathbf{m}_k + \frac{2}{L} \boldsymbol{\Gamma}^T (D - \boldsymbol{\Gamma} \mathbf{m})], \quad (3)$$

where  $\mathbf{m}_k$  is the solution or the deblended model at  $k_{th}$  iteration,  $T_{\tau,P}$  is the thresholding function depending on the threshold  $\tau$  and norm  $P$ ,  $L$  is a factor proportional to the blending fold and  $\boldsymbol{\Gamma}^T$  is the pseudo deblending operator. The sparsity-promoted transformation  $S^{-1}$  is a 3D FK transform done in optimally sized 3D windows to ensure linear representation of events. The threshold  $\tau$  descends exponentially with the number of iterations. The subtraction of the re-blended model from the recorded data is performed in real space, while the thresholding is done in the sparse 3D FK domain across all windows.

High blend-fold in OBN acquisition demands a more stable and accurate algorithm, so we parameterize the regularization norm to enhance our ISTA algorithm on those aspects. In practice, L<sub>1</sub> norm always converges but the solution is not necessarily the best one, while L<sub>0</sub> norm, which has the clearest physical meaning in sparsity, doesn't always give a convergent solution. So, the norm is continuously tuned to ensure both convergence and precision at the same time.

In inversion computation, it is a normal approach to use optimal 3D local windows to improve linearity and sparsity in the transformed domain. In our implementation, the time-variant windows are customized to the local events. For example, in areas where strong steep blending noise and weak flat desired signal overlay each other we use larger windows than in other places to promote the weak signal in the sparse domain. This helps promote the desired signal in the deblended model.

Another idea to preserve the weak signal concealed by strong blending noise is that we only work on strong signal regions in the early iterations. When weak events are overlain with strong blending noise, there is high chance that noise will leak into the signal model. So, we skip those areas during early iterations. Once we have generated a high-precision model of strong signal, the strong blending noise is automatically removed from the blended data, as this is strong signal from other sources. Therefore, it is more reliable to model the weak signal in later iterations after some of the blending noise has been removed.

It is also worth mentioning that it is beneficial to flatten the data before deblending, because unlike in the channel domain of streamer data, we do not have relatively flat events in receiver domain of OBN acquisition. It is also important to clean up the model at the end of each iteration to improve the accuracy of modeling. Although ISTA allows some inaccuracy at early iterations, it is still better to reduce noise leakage.

### NOAKA OBN

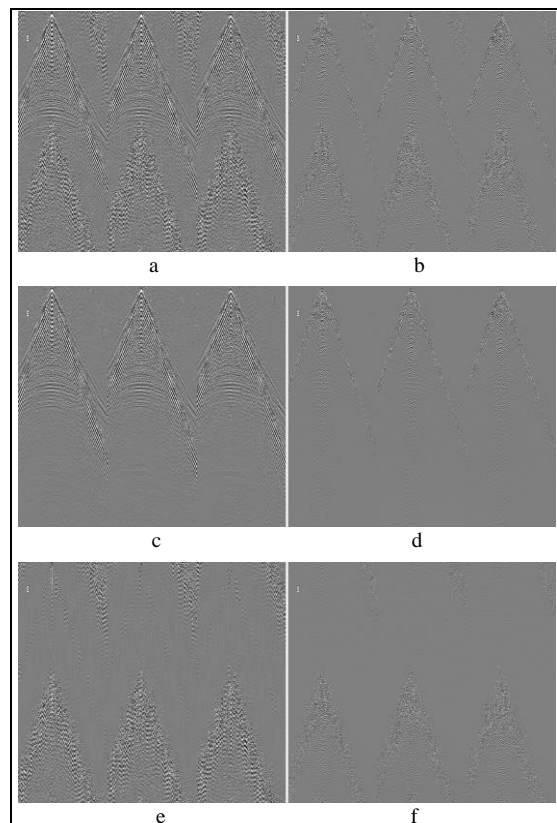


Figure 1: Data in common receiver gather (7s): a) input P wave; b) input Vz component; c) deblended P wave; d) deblended Vz component; e) difference of Fig. 1(a) and 1(c); f) difference of Fig. 1(b) and 1(d). (Data courtesy of TGS)

The TGS NOAKA OBN 2021 survey covers a polygon on the Norwegian continental shelf, acquired using a single vessel with triple sources, shot in a flip-flop-flap way. The shot interval is 8.33m, with a dither time of  $\pm 400$ ms. Shot line spacing is 50 meters with a shot spacing along the shot line of 25 meters. Receiver line separation is 300m and the receiver interval is 50m. The maximum offset is 4km. Sample rate is 2ms and initial record length is 7s. The shot halo is about 4km.

## Sub-L<sub>1</sub> Norm Regularized Inversion Deblending in Local 3D FK Domain for OBN Data

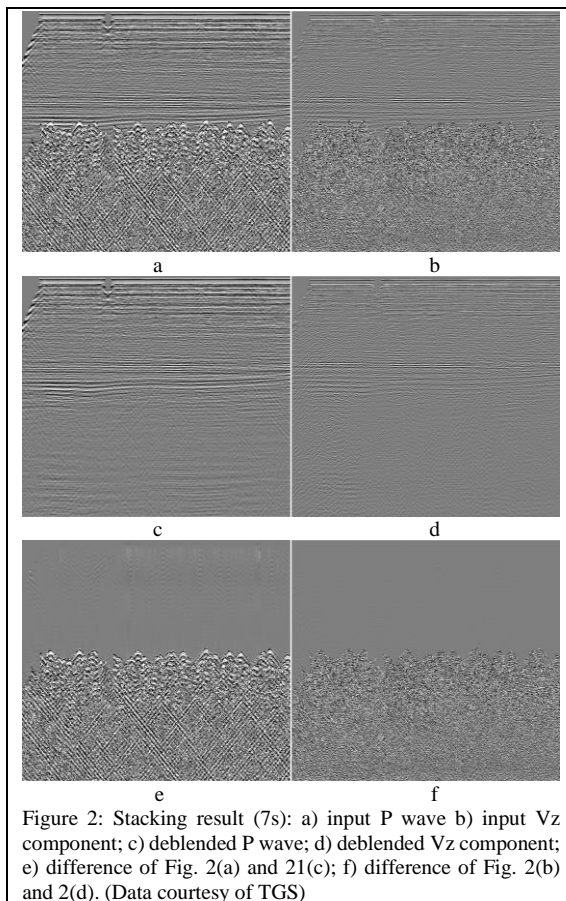


Figure 2: Stacking result (7s): a) input P wave b) input Vz component; c) deblended P wave; d) deblended Vz component; e) difference of Fig. 2(a) and 21(c); f) difference of Fig. 2(b) and 2(d). (Data courtesy of TGS)

We applied our new inversion deblending methods on the data and present both the P wave and Vz component results in Figure 1. The strong blending noise seen above the direct arrival energy and in the central area in Fig. 1 (c) and (d) are removed, while signal energy is preserved with high precision. Fig. 1(e) and (f) indicates direct arrival and refractions are fully recovered without harm, while overlaid erratic blending noise is removed. The underlying weak flat reflections are either revealed or have improved continuity.

The images in Fig. 2 show stack results before and after deblending for the P wave and Vz components. The first order multiples are now clearly visible and even second order multiples are apparent when blending noise is removed. The primaries are preserved with high accuracy across the whole line.

### Utsira OBN

Utsira is a long offset OBN survey located in the North Sea over the Utsira High (Ramirez et al., 2020). The data was

acquired with the geometry of 300m receiver line spacing and 50m receiver station interval. The source lines are parallel to the receiver lines using 50m source line spacing and 25m shot interval. Two source vessels with triple source configurations were used to shoot the data in 2018, with the number of source vessels increased to three later in the campaign.

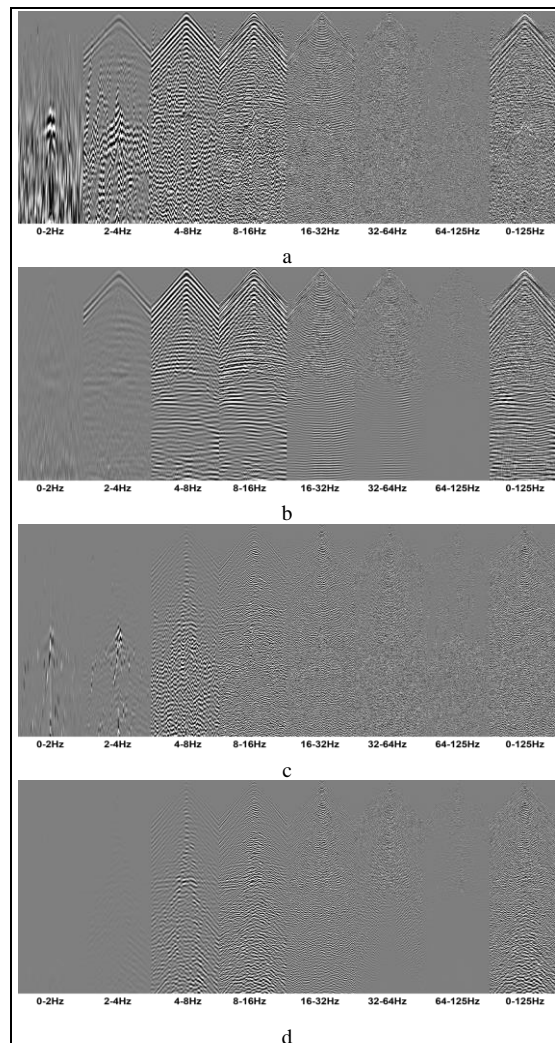


Figure 3: Data in common receiver gather from different octaves (6s): a) Hydrophone input; b) Hydrophone deblended; c) Geophone input; d) Geophone deblended. (Data courtesy of TGS)

In Figure 3, we show our deblending results in common receiver gather from different octaves for both hydrophone data and geophone data. In the 2-4Hz octave, weak reflection events can be seen down to 6s in both the hydrophone and geophone deblended models. Even in the sub 2Hz octave,

## Sub-L<sub>1</sub> Norm Regularized Inversion Deblending in Local 3D FK Domain for OBN Data

signal is evident; the surface wave can be seen to 3.5s in the hydrophone model.

Diving wave energy is of interest to us as this project is mainly aimed at FWI velocity model updates. The diving wave is largely interfered by erratic blending noise prior to

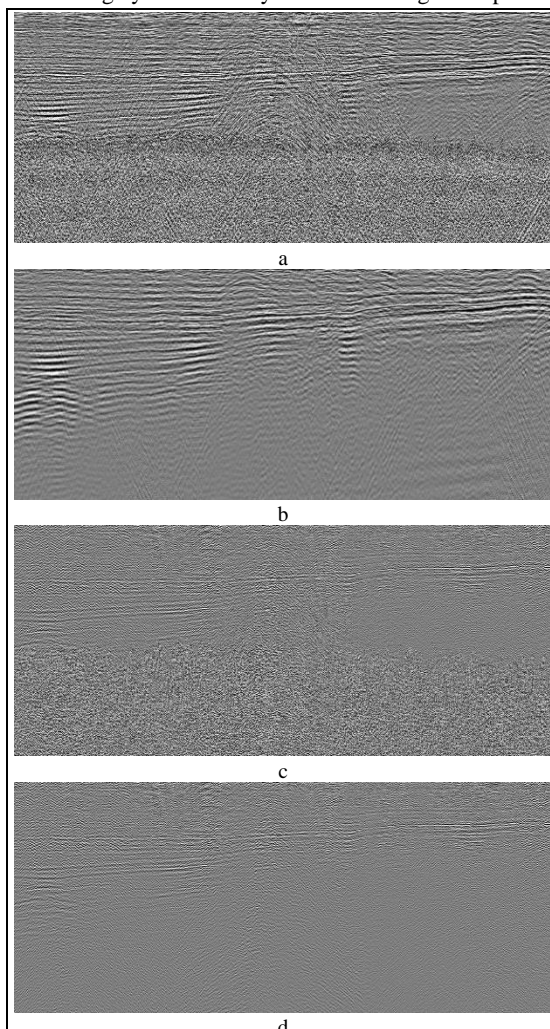


Figure 4: 3D Stacking Results (4.8s): a) Hydrophone input; b) Hydrophone deblended; c) Geophone input; d) Geophone deblended. (Data courtesy of TGS)

deblending but is recovered precisely during the inversion deblending process. The noticeable separation of diving wave from direct arrival in the 4-8Hz and 8-16Hz octaves shown in Fig.3(b) and more so in Fig.3(d) indicate the prospective benefits to FWI.

3D stacking is performed on the whole sequence line before and after deblending and the comparison is summarized in

Figure 4. Blending noise in Fig. 4(a) and 4(c) in the shallow and deep section is removed and the fine structure behind it is revealed as shown in Fig. 4(b) and 4(d). The amplitudes of the primary events are not compromised and are preserved consistently across the whole line in both the hydrophone and geophone deblended models. Additionally, in both cases, the subtle diffraction tails are either uncovered or improved after deblending.

### Conclusions

High blend-fold in OBN simultaneous source acquisition presents a challenge on the stability and accuracy of our legacy inversion deblending algorithm. We have developed a new sparse inversion deblending method to solve the problem and application on the NOAKA and Utsira OBN projects achieve great results.

This new inversion deblending method takes advantage of several existing mathematical tools and integrates them into one powerful module. We use the popular ISTA method as a solver and use sub-L<sub>1</sub> norm to regularize the least square problem of deblending. The combination of the two effectively ensures a stable convergence into a sparse solution in the local 3D FK domain. The parameterization of norm allows us to push the modeling accuracy even higher without causing divergence, which occurs when the norm gets too small (close to 0.5).

Time-variant local 3D windows enhance event linearity and help reveal the weak flat events which are masked by strong blending noise in OBN data.

Both field examples show the efficacy of our new method. The deblended gather hydrophone and geophone results, for NOAKA and Utsira, demonstrate this method accurately recovers the weak flat events in heavily contaminated areas and is precise in preserving the direct arrivals and diving waves. The stacking results show consistent accuracy through the whole line. This method successfully meets the challenges raised by OBN simultaneous source acquisition. Further, the sub-L<sub>1</sub> norm regularization can be used with any other sparsity-promoted transforms, such as the  $\tau$ - $p$ , wavelet and curvelet transform, to help improve inversion deblending or other inversion problems.

### Acknowledgement

We thank Zhigang Zhang and Adriana Citlali Ramirez for technical discussions, Eddie Cho, Matt Hawke and Greg Szumski for producing the stack trials, and Sarah Spoores for her support and suggestions. We also thank TGS for permission to show the field examples and publish this work. Finally, we acknowledge our joint venture partners on the Utsira OBN project, Axxis Multi-Client.

## REFERENCES

- Abma, R., Q. Zhang, A. Arogunmati, and G. Beaudoin, 2012, An overview of BP's marine independent simultaneous source field trials: 82nd Annual International Meeting, SEG, Expanded Abstracts, doi: <https://doi.org/10.1190/segam2012-1404.1>.
- Abma, R. L., and M. Foster, 2020, Simultaneous source seismic acquisition: SEG, Geophysical Developments Series, **18**, 43–104.
- Abma, R. L., D. Howe, M. Foster, I. Ahmed, M. Tanis, Q. Zhang, A. Arogunmati, and G. Alexander, 1998, Independent simultaneous source acquisition and processing: *Geophysics*, **63**, 2120–2128, doi: <https://doi.org/10.1190/geo2015-0078.1>.
- Abma, R. L., T. Manning, M. Tanis, J. Yu, and M. Foster, 2010, High quality separation of simultaneous sources by sparse inversion: 72nd Annual International Conference and Exhibition, EAGE, Extended Abstracts, cp-161, doi: <https://doi.org/10.3997/2214-4609.201400611>.
- Abma, R. L., and J. Yan, 2009, Separating simultaneous sources by inversion: 71st Annual International Conference and Exhibition, EAGE, Extended Abstracts, doi: <https://doi.org/10.3997/2214-4609.201400403>.
- Akerberg, P., G. Hampson, J. Rickett, H. Martin, and J. Cole, 2008, Simultaneous source separation by sparse radon transform: 78th Annual International Meeting, SEG, Expanded Abstracts, 2801–2805, doi: <https://doi.org/10.1190/1.3063927>.
- Beasley, C. J., R. E. Chambers, and Z. Jiang, 2018, A new look at simultaneous sources: 88th Annual International Meeting, SEG, Expanded Abstracts, R335–R344, doi: <https://doi.org/10.1190/1.1820149>.
- Berkhout, A. J., 2008, Changing the mindset in seismic data acquisition: *The Leading Edge*, **27**, 924–938, doi: <https://doi.org/10.1190/1.2954035>.
- Chen, Y., S. Fomel, and J. Hu, 2006, Iterative deblending of simultaneous-source seismic data using seislet-domain shaping regularization: *Geophysics*, **71**, no. 1, N1–N9, doi: <https://doi.org/10.1190/geo2013-0449.1>.
- Kumar, A., and G. Hampson, 1997, An inversion-based deblending solution: 67th Annual International Meeting, SEG, Expanded Abstracts, 895–905, doi: <https://doi.org/10.1190/segam2020-3427002.1>.
- Liu, Z., B. Wang, J. Specht, J. Sposito, and Y. Zhai, 2014, Enhanced adaptive subtraction method for simultaneous source separation: 84th Annual International Meeting, SEG, Expanded Abstracts, 4065–4069, doi: <https://doi.org/10.1190/segam2014-1510.1>.
- Mahdad, A., P. Doulgeris, and G. Blacquiere, 2011, Separation of blended data by iterative estimation and subtraction of blending interference noise: *Geophysics*, **76**, no. 3, Q9–Q17, doi: <https://doi.org/10.1190/1.3556597>.
- Masoomzadeh, H., S. Baldock, and Z. Liu, 2018, Deblending continuous records by sparse inversion of energetic and coherent surfaces: 88th Annual International Meeting, SEG, Expanded Abstracts, 4065–4069, doi: <https://doi.org/10.1190/segam2018-2995944.1>.
- Masoomzadeh, H., S. Baldock, Z. Liu, H. Roende, C. Mason, and H. Pal, 2019, Deblending of long-offset OBN data for velocity model building by sparse inversion of hyperboloidal components: 89th Annual International Meeting, SEG, Expanded Abstracts, 4053–4057, doi: <https://doi.org/10.1190/segam2019-3216531.1>.
- Moore, I., B. Dragoset, T. Ommundsen, D. Wilson, C. Ward, and D. Eke, 2008, Simultaneous source separation using dithered sources: 78th Annual International Meeting, SEG, Expanded Abstracts, 2806–2809, doi: <https://doi.org/10.1190/1.3063928>.
- Peng, C., and J. Meng, 2016, Inversion-based 3D deblending of towed-streamer simultaneous source data using sparse tau-P and wavelet transforms: 86th Annual International Meeting, SEG, Expanded Abstracts, 4607–4611, doi: <https://doi.org/10.1190/segam2016-13866688.1>.
- Qu, S., H. Zhou, R. Liu, Y. Chen, S. Zu, S. Yu, J. Yuan, and Y. Yang, 2016, Deblending of simultaneous-source seismic data using fast iterative shrinkage-thresholding algorithm with firm-thresholding: *Acta Geophysica*, **64**, 1064–1092, doi: <https://doi.org/10.1515/acgeo-2016-0043>.
- Ramirez, A. C., F. Anderson, B. Kjølhamar, and J. Robertsson, 2021, A deca-source towed marine test — An innovative and efficient design: First International Meeting for Applied Geoscience & Energy, SEG, Expanded Abstracts, 66–70, doi: <https://doi.org/10.1190/segam2021-3594454.1>.
- Ramirez, A. C., S. Baldock, D. Mondal, J. Gromotka, and M. Hart, 2020, Long offset ocean bottom node full-waveform inversion and multi-azimuth tomography for high-resolution velocity model building: North Sea, Utsira High: 90th Annual International Meeting, SEG, Expanded Abstracts, 750–754, doi: <https://doi.org/10.1190/segam2020-3428806.1>.
- Sun, J., Z. Liu, M. Guo, A. Willis, N. Pralica, and L. Gaboli, 2022, Sufficient data extension and sub-L1 norm regularization in 3D inversion-based deblending: 84th Annual International Conference and Exhibition, EAGE, Extended Abstracts, doi: <https://doi.org/10.3997/2214-4609.202210923>.
- Xuan, Y., R. Malik, Z. Zhang, M. Guo, and Y. Huang, 2020, Deblending of OBN ultralong-offset simultaneous source acquisition: 90th Annual International Meeting, SEG, Expanded Abstracts, 2764–2768, doi: <https://doi.org/10.1190/segam2020-3428390.1>.
- Zhan, C., R. Malik, J. Specht, Z. Liu, and D. Teixeira, 2015, Deblending of continuously recorded OBN data by subtraction integrated with a median filter: 85th Annual International Meeting, SEG, Expanded Abstracts, 4673–4677, doi: <https://doi.org/10.1190/segam2015-5827990.1>.